International Journal of Pharmaceutics 400 (2010) 251–259

Contents lists available at ScienceDirect

International Journal of Pharmaceutics

journal homepage: www.elsevier.com/locate/ijpharm

Pharmaceutical Nanotechnology

Mixed backbone antisense glucosylceramide synthase oligonucleotide (MBO-asGCS) loaded solid lipid nanoparticles: In vitro characterization and reversal of multidrug resistance in NCI/ADR-RES cells

Akhtar Siddiqui, Gauri Anand Patwardhan, Yong-Yu Liu, Sami Nazzal*

Department of Basic Pharmaceutical Sciences, College of Pharmacy, University of Louisiana at Monroe, Monroe, LA 71209-0497, United States

ARTICLE INFO

Article history:
Received 29 May 2010
Received in revised form 4 August 2010
Accepted 27 August 2010
Available online 15 September 2010

Keywords:
Solid lipid nanoparticle
Antisense oligonucleotide
Stability
Cancer therapy
Drug delivery

ABSTRACT

In this study, solid lipid nanoparticles (SLN) loaded with MBO-asGCS oligonucleotide were prepared, characterized and evaluated for cytotoxicity against NCI/ADR-RES human ovary cancer cells. Two types of cetyltrimethyl ammonium bromide (CTAB) stabilized SLN, with or without ceramide VI, were prepared by mixed homogenization/ultrasonication technique. Complexes were characterized for size, zeta-potential, and stability in biorelevant media and against DNaseI activity. Binding and release studies were further confirmed by gel electrophoresis. Cytotoxicity of the SLN against NCI/ADR-RES cells was evaluated by quantizing ATP. SLN with ceramide VI had lower particle size (74.6 nm) with improved stability in RPMI media when compared to reference SLN without ceramide VI (167.16 nm). Both SLN however had similar cytotoxicity profile with an optimum binding at CTAB to MBO-asGCS ratio of 6:1. Blank SLN, and free MBO-asGCS in the presence and absence of free doxorubicin had insignificant effect on the viability of NCI/ADR-RES cells. However, when cells were concurrently treated with MBO-asGCS loaded SLN and free doxorubicin, cell viability significantly decreased to approximately 12%. These results suggested that SLN enhanced internalization and uptake of MBO-asGCS oligonucleotide, which led to the downregulation of GCS and subsequently reversing the resistance of the cells to doxorubicin.

© 2010 Elsevier B.V. All rights reserved.

1. Introduction

Development of multidrug resistance (MDR) in cancer cells is a frequent cause of treatment failure with conventional chemotherapeutics. MDR may be developed from over-expression of Pgp, increased DNA damage repair, altered target sensitivity, decreased apoptotic response, aberrant signal transduction pathways, or elevated level of glycolipids (Norris-Cervetto et al., 2004; Lucci et al., 1999; Cabot et al., 1999; Gouaze et al., 2004). Glycolipids are the structural elements of the biological membrane and have been implicated in cell proliferation, differentiation and oncogenic transformation (Liu et al., 1999). Growing evidence has also been accumulated regarding the role of glycolipids in the development of MDR, especially in adriamycin resistant cancer cells (Liu et al., 2000, 2001; Gouaze et al., 2005; Gouaze-Andersson and Cabot, 2006). According to Liu et al. (1999, 2004), chemotherapeutic agents may induce the production of glucosylceramide synthase (GCS), which glycosylates the pro-apoptotic ceramide to glucosylceramide, and the accumulation of glucosylceramide leads to cell proliferation and resistance. Therefore, downregulating and/or inhibiting GCS have been suggested as a therapeutic approach to overcome MDR and enhance the cytotoxicity of the conventional chemotherapeutics (Liu et al., 2004).

Various modalities have been employed in order to manage the cellular level of glucosylceramide synthase, such as the use of ceramide analogs, GCS inhibitors, GCS specific siRNA, and GCS antisense oligonucleotide (asGCS) (Gouaze-Andersson and Cabot, 2006). Whereas ceramide analogs and GCS inhibitors were found to have undesirable and non-specific effects, the use of siRNA and GCS antisense approach is devoid of them (Liu et al., 2004). Although siRNA was shown to have better gene knock-down efficacy than GCS antisense, it suffers from cost and handling constrains (Grünweller et al., 2004). GCS antisense, on the other hand, was viewed as a promising molecular medicine when, for the first time, FDA gave marketing approval to the phosphorothioate-based oligonucleotide injection (Vitravene®) as a treatment modality for ophthalmic infection to cytomegalovirus in HIV patients (Bijsterbosch et al., 2002). In reality, the therapeutic potential of Vitravene® would not have been the same had it been administered systemically (Yessine et al., 2006; Bondi et al., 2007; Asasutjarit et al., 2007). Therefore, the real potential of oligonucleotide can only be realized when it reaches its target site in therapeutically

* Corresponding author at: Department of Basic Pharmaceutical Sciences, College of Pharmacy, University of Louisiana at Monroe, 1800 Bienville Drive, Monroe, LA 71201, United States. Tel.: +1 318 342 1726; fax: +1 318 342 1737.
E-mail address: nazzal@ulm.edu (S. Nazzal).

0378-5173/$ – see front matter © 2010 Elsevier B.V. All rights reserved.
doi:10.1016/j.ijpharm.2010.08.044

efficient concentration. Upon systemic administration, however, oligonucleotides are subjected to nucleases, immune-surveillance, and endosome-lysosome trafficking before they reach their target site (Asasutjarit et al., 2007; Leonetti et al., 2001; Vogel et al., 2005). Therefore, a delivery system is required to surpass systemic and intracellular challenges and deliver these molecules to their target site in a therapeutically efficient concentration.

Several non-viral systems have been used for the systemic administration of genetic materials. In these systems cationic peptides, dendrimers, polycationic polymers and cationic lipids are used to interact and bind to negatively charged DNA/RNA/oligonucleotide (Tabatt et al., 2004a,b; Bondi et al., 2007). In this arena, cationic liposomes were on the forefront as a delivery vehicle until the use of solid lipid nanoparticles (SLN) was reported in 2001 by Olbrich et al. The very common architecture of SLN is a solidifiable core lipid which accommodates a hydrophobic drug. SLN were shown to offer several technological advantages, which include a reduced effect of ionic strength on stability, possible targeting by surface modification, protection of incorporated drug, high drug loading, use of pharmaceutically acceptable material, lack of usage of organic solvent, and the possibility of steam sterilization and lyophilization (Vighi et al., 2007; Tabatt et al., 2004a,b).

For the production of cationic SLN, dispersion of solid lipids, such as cetyl-palmitate and emulsifying wax, is stabilized by cationic lipids and surfactants (Bondi et al., 2007; Vighi et al., 2007; Tabatt et al., 2004a,b; Asasutjarit et al., 2007; Pozo-Rodríguez et al., 2007; Montana et al., 2007; Cui and Mumper, 2002a,b). In the present study cationic SLN were prepared from stearyl alcohol and cetyltrimethyl ammonium bromide (CTAB), with and without a phyto-ceramide (ceramide VI), for the delivery of mixed backbone asGCS (MBO-asGCS). A phyto-ceramide was selected as a part of the core lipid because caramides are known for their physiological roles in cell adhesion and epidermal differentiation and as second signal messengers in stress induced apoptosis (Hatziantoniou et al., 2007). MBO-asGCS on the other hand is a second generation oligonucleotide where part of the deoxyribosyl PS backbone in the antisense molecule was replaced with other type of backbone modifications. These modifications provide nuclease resistance and RNaseH activation-induced digestion of the duplexed RNA. The MBO-asGCS used in this study was extensively investigated for its efficacy on NCI/ADR-RES human ovary cancer cell line by our group (Liu et al., 2004). In order to realize its clinical potential, cationic SLN were prepared as potential delivery system for the systemic administration of MBO-asGCS. The objectives of this study were therefore to (a) prepare MBO-asGCS SLN, (b) characterize the nanoparticles with respect to particle size, zeta-potential, and binding efficiency, and (c) test the antiproliferative effect of the MBO-asGCS SLN against adriamycin resistant NCI/ADR-RES human ovary cancer cells.

2. Materials and methods

2.1. Materials

Stearyl alcohol and cetyltrimethyl ammonium bromide (CTAB) were purchased from Tokyo Chemical Industry Co (Portland, OR). Ceramide VI (Fig. 1) was a generous gift from Evonik (Norwalk, CT). The primer and Lipofectamine™ were purchased from Invitrogen (Carlsbad, CA). MBO-asGCS (mixed backbone antisense glucosylceramide synthase oligonucleotide) was purchased from Integrated DNA Technologies (Coralville, IA). Materials for TAE buffers (Tris, EDTA (0.5 M), and glacial acetic acid were supplied by Fisher biotech (Springfield, NJ). Fetal bovine serum was purchased from Hyclone (Logan, UT). Sodium lauryl sulfate was provided by Spectrum (Gardena, CA). DNase I and material used for phosphate and acetate buffer were obtained from Sigma (St. Louis, MO). Agarose for gel electrophoresis was purchased from EMD (Gibbstown, NJ). Purified water for the dispersion was obtained from Nanopure ultra water system.

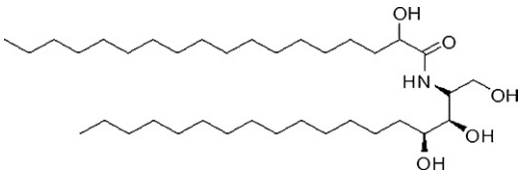

Fig. 1. Structural formula of ceramide VI, which consists of a phytosphingosine backbone acylated with a long chain alpha-hydroxy stearic acid.

2.2. Preparation of cationic SLN

Cationic SLN for binding the negatively charged MBO-asGCS was prepared by modified microemulsion method combining shear and ultrasonic homogenization techniques. Two types of SLN nanoparticles were prepared from either stearyl alcohol/CTAB at 2:1 weight ratio (SLN1) or stearyl alcohol/ceramide VI/CTAB at 1:1:1 weight ratio (SLN2). Stearyl alcohol at a concentration of 0.5% (w/w) was first heated to 90 °C. Then a preheated aqueous solution of CTAB or CTAB/ceramide VI blend was transferred to the molten stearyl alcohol. This mixture was then homogenized for 5 min at 20,000 RPM using UltraTurax T8 (IKA, Wilmington, NC). Thereafter, the crude o/w emulsion was ultrasonicated for 10 min at 40% power and 60% pulsar rate using probe sonicator (Model 150 V/T, Biologics, Inc., Manassas, VI). SLN were formed by cooling the emulsion at ambient conditions to room temperature.

2.3. Particle size and zeta-potential measurement

The mean particle size of the SLN was measured by photon correlation spectroscopy using Nicomp™380 ZLS. The size was recorded at 25 °C by scattering light at an angle of 90 degrees for 90 s with viscosity and dielectric constant of the medium 1.33 and 78.5, respectively. As recommended by the manufacturer, SLN formulations were diluted with Nanopure water in order to avoid multiple scattering and to achieve the scattering intensity of 300 kHz. The intensity-weighted mean diameter of the particles was calculated based on Stokes–Einstein law by curve fitting of the correlation function. Zeta-potential of the SLN was measured using the same instrument (Nicomp™380 ZLS) under zeta mode. The sample was diluted with Nanopure water and zeta-potential was measured using the Helmholz–Smoluchowsky equation.

2.4. Transmission electron microscopy

The morphology of the SLN1 and SLN2 was visualized by transmission electron microscopy. A drop of the SLN dispersion was applied to a carbon-coated copper grid. The samples were then negatively stained with 2% (w/v) of phosphotungstic acid. After 5 min, excess fluid was removed with a filter paper and the grid was allowed to air dry. Samples were then visualized by a transmission electron microscope (model JEM-1011, Joel, Tokyo, Japan) and photographs were captured at suitable magnification.

2.5. Stability of SLN

Particle size-growth was taken as an index of SLN-stability. Stability of SLN aqueous dispersions was carried out by measuring the change in particle size with time over four weeks for samples stored at room temperature, refrigeration, and at 37 °C.

Table 1
Composition and physical properties of the SLN ($n = 3$).

SLN	Composition (ratio w/w)	Particle size (nm)* (mean ± SD)	Polydispersity index (PI) (mean ± SD)	Zeta-potential (+mV)** (mean ± SD)
SLN1	Stearyl alcohol:CTAB 2:1	167.16 ± 1.62	0.18 ± 0.01	39.31 ± 0.28
SLN2	Stearyl alcohol:ceramide VI:CTAB 1:1:1	74.6 ± 1.15	0.21 ± 0.02	35.82 ± 2.33

* p-value < 0.0001.
** p-value = 0.062.

2.6. Preparation of MBO-asGCS SLN complexes

Before complexing MBO-asGCS with the SLN, the formulations were sterilized in biological hood using 0.22 μm PVDF syringe filter. After filtration, MBO-asGCS at various ratios of CTAB to MBO-asGCS ranging from 0.62:1 to 25:1 (w/w) was added to the aqueous SLN dispersion. The mixtures were immediately vortexed for 20 s to minimize cross-binding of one MBO-asGCS with multiple SLN leading to aggregate formation. After vortexing, the formulations were allowed to stand for half an hour at room temperature to allow the MBO-asGCS to bind with the SLN.

2.7. Agarose gel electrophoresis

MBO-asGCS SLN complexes were analyzed by gel electrophoresis using 1% agarose gel. Loading buffer was used to ensure settling of the complex in the well. The bands were observed after 5, 10, 15, and 20 min with Alfa Innotech transilluminator using ethidium bromide (AlphaInnotech Corp., San Leandro CA).

2.8. DNase I digestion assay

Since genetic materials are susceptible to enzymatic degradation, the primer–SLN complex was subjected to DNaseI activity to evaluate whether the complex could protect the primer. In this study, a primer was used since the MBO-asGCS is resistant to DNase by design. The primer/SLN at ratios of 1:6 (w/w) was mixed with DNaseI (2 μl). After 10 min, the DNaseI stabilizing buffer supplied with the DNaseI kit (2 μl) was added to terminate the DNaseI activity and the samples were analyzed by gel electrophoresis. In order to confirm the integrity of the primer complex with the SLN, sodium laurayl sulfate (SLS) at 1% concentration was added to the SLN dispersion to force the release of the bound primer. After SLS addition, the complexes were subjected to gel electrophoresis and the image of the gel was captured.

2.9. Oligonucleotide release study

MBO-asGCS SLN complexes were treated with either buffer at pH 7.4, 7.2 and 4.5, 10% FBS in 150 mM NaCl, 150 mM NaCl, or 10% lactose. After 30 min, gel electrophoresis was performed and images were captured using the above described procedure.

2.10. Cell culture and reagents

Drug resistant NCI/ADR-RES human ovary cancer cell line was kindly provided by Dr. Kenneth Cowan (UNMC Eppley Cancer Center, Omaha, NE) and Dr. Merrill Goldsmith (National Cancer Institute, Bethesda, MD). Cells were cultured in RPMI-1640 medium (with 10% fetus bovine serum, 100 units/ml penicillin, 100 μg/ml streptomycin, 584 mg/l L-glutamine) and maintained in an incubator humidified with 95% air and 5% CO_2 at 37 °C.

2.11. Cell viability assay

This assay was performed to screen non-specific toxicity of the formulations and to investigate cell apoptosis resulting from the MBO-asGCS SLN complex. Cell viability was determined by quantizing ATP, an indicator of live cells, using the CellTiter-Glo luminescent cell viability assay kit (Promega, Madison, WI) as described by Patwardhan et al. (2009). Briefly, cells (4000 cells/well) were plated in 96-well plates with 10% FBS RPMI-1640 medium overnight. Cells were either treated with oligo-free SLN1 and SLN2, or SLN complexes containing 100 nM MBO-asGCS. Cells treated with Lipofectamine™ 2000 (Invitrogen, Carlsbad, CA) or lipofectamine plus MBO-asGCS were used as controls. A separate set of studies were performed in which doxorubicin (5 μM) was added to all treatments. After treatment, cells were kept for 72 h after which cell viability was determined by measuring luminescent ATP in a Synergy HT microplate reader (BioTek, Winnooski, VT) following incubation with CellTiter-Glo reagent.

2.12. Statistical analysis

Data were analyzed by the ANOVA. Linear contrast was used whenever necessary to distinguish the mean differences in particle size and zeta-potential. Bonferroni method of multiple comparisons was performed to interpret cell viability data. Differences were considered significant if $p < 0.05$.

3. Results

3.1. Particle size and zeta-potential measurement

SLN1 and SLN2 (Table 1) were prepared by a modified microemulsion method by subjecting the samples to shear homogenization and sonication. The average particle size of SLN2 with 50% (w/w) of the total core lipid substituted with ceramide was significantly lower than that of SLN1 (p-value < 0.0001). The average particle size of SLN1 and SLN2 was 167.2 and 74.6 nm, and their polydispersity index (PI) was 0.18 and 0.21, respectively. The average zeta-potential of SLN1 and SLN2 was (+) 39.31 and 35.82 mV, respectively. High surface charge on SLN indicated that CTAB was inserted in the core lipids as reported by Bondi et al. (2007). The overall zeta-potential however was not significantly different (p-value = 0.062). A representative TEM image of the nanoparticles is given in Fig. 2.

3.2. Stability of SLN at different storage conditions

Aqueous SLN dispersions were stored at room temperature, in the refrigerator, and at 37 °C for four weeks. The average particle size of SLN1 after four weeks of storage in refrigeration, room temperature, and 37 °C was 160.0, 205.9 and 856.0 nm whereas the average particle size of SLN2 was 76.8, 95.5, and 81.1 nm, respectively (Fig. 3). By applying linear contrast on the storage data, particle size of SLN1 significantly increased when the dispersions were stored at 37 °C, whereas no significant differences in particle size was observed when stored at room temperature and

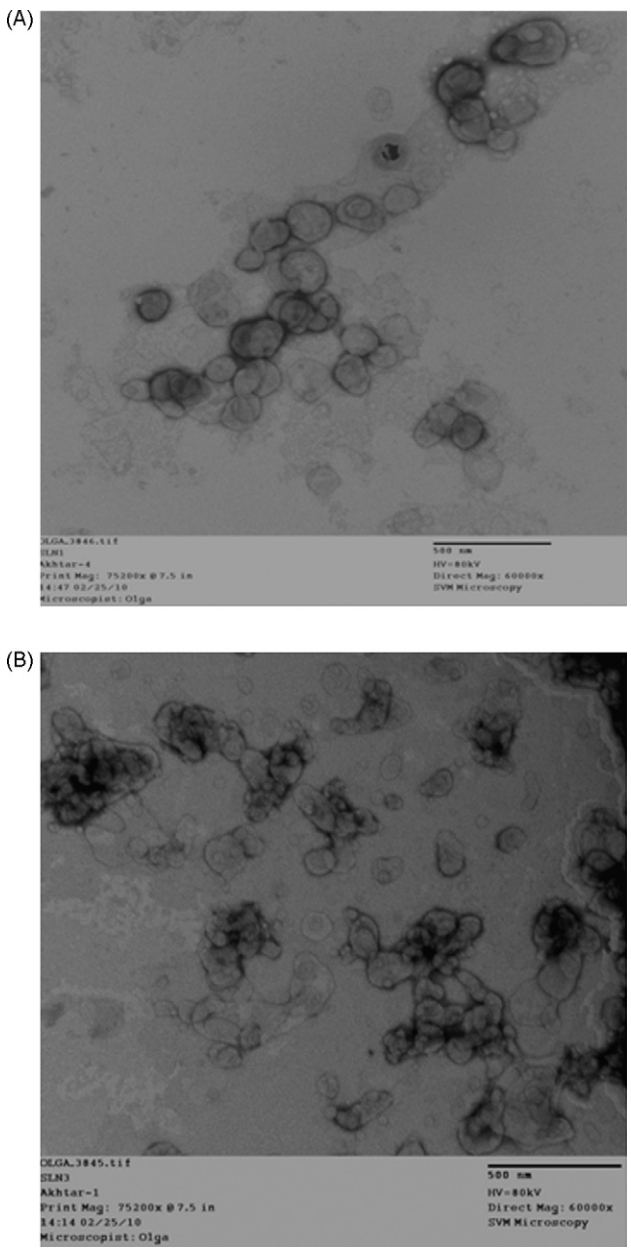

Fig. 2. Representative transmission electron micrographs (TEM) of (A) SLN1 and (B) SLN2.

refrigerated. When similar treatment was applied to SLN2 data, no significant increase in particle growth was observed when the samples were stored at elevated temperature (37 °C), which may be attributed to the stabilizing effect of ceramide in the nanoparticles. After four weeks of storage at room temperature the zeta-potential of SLN1 and SLN2 was (+) 38.8 and 35.0 mV, respectively.

3.3. Determination of optimal MBO-asGCS to SLN binding ratios

Complexes at various ratios of CTAB to MBO-asGCS were prepared as described in Section 2 and their zeta-potential was measured. Zeta-potential values (Fig. 4) were found to increase with an increase in CTAB to MBO-asGCS ratio and plateaued at an approximate ratio of 10:1 (w/w). The drift in zeta-potential from a negative to a positive value was due to the gradual neutralization of the negatively charged MBO-asGCS by cationic SLN. When completely neutralized, an increase in the concentration of cationic

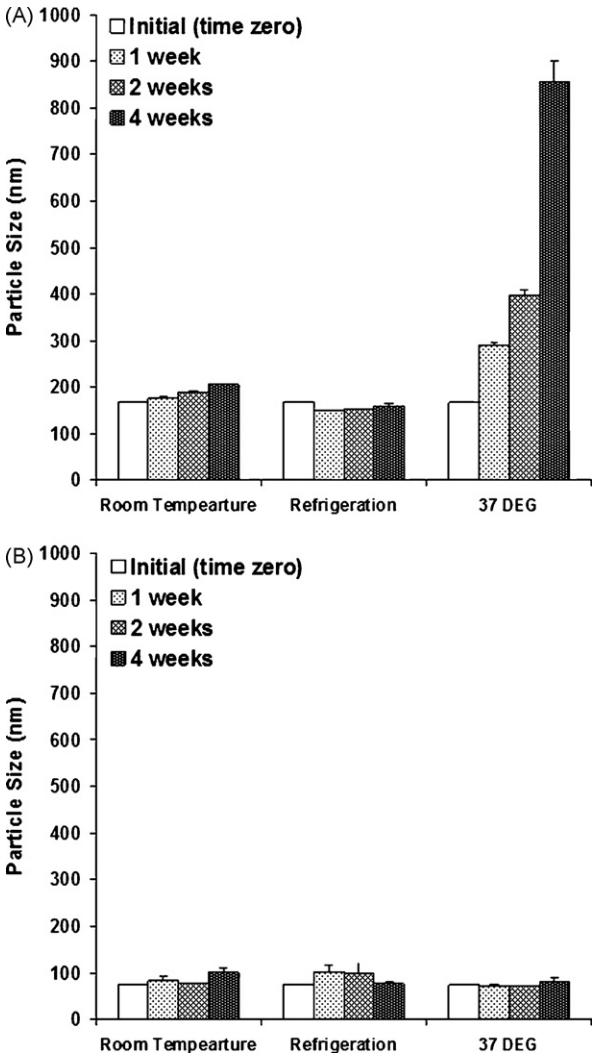

Fig. 3. Stability of (A) SLN1 and (B) SLN2 with respect to particle size when the nanoparticles were stored at controlled room temperature, refrigeration, and 37 °C for up to four weeks.

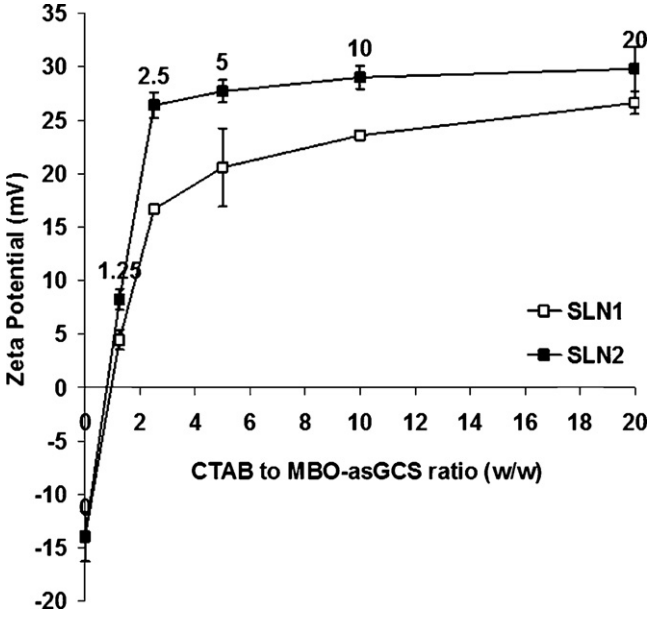

Fig. 4. Effect of CTAB to MBO-asGCS ratio on the zeta-potential of SLN1 and SLN2 nanoparticles.

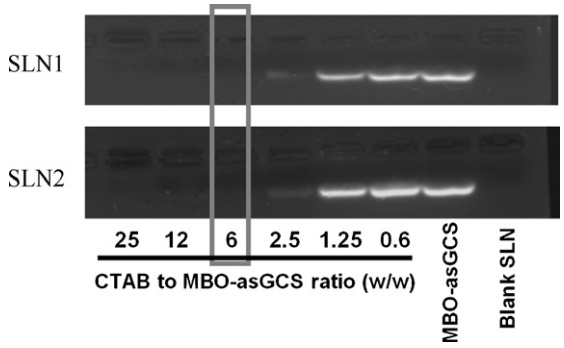

Fig. 5. Binding of MBO-asGCS to SLN1 and SLN2. 2 μg of MBO-asGCS was incubated for 30 min with increasing amount of cationic CTAB, which was used as an indirect measure of the total nanoparticle concentration. The box indicates the CTAB to MBO-asGCS ratio which was used in subsequent studies. It also represents the threshold at which complete MBO-asGCS binding to SLN was first observed.

SLN did not show significant increase in zeta-potential. Therefore, complete charge neutralization, which indicates complex formation, occurred at CTAB to MBO-asGCS ratios between 1.25:1 and 10:1 (w/w).

3.4. Agarose gel electrophoresis

In order to confirm complex formation as predicted by the zeta-potential data, agarose gel electrophoresis was performed on a series of complexes (Fig. 5). As seen from the figure, no band appeared for SLN1 and SLN2 complexes at CTAB to MBO-asGCS ratios at or greater than 6:1 (w/w). Based on zeta-potential and gel electrophoresis data, a CTAB to MBO-asGCS ratio of 6:1 (w/w) was selected for subsequent complex characterization and cytotoxicity. This ratio was taken to ensure complete binding and to avoid the presence of free MBO-asGCS due to subtle differences in complex processing, which may affect comparative interpretation of data with respect to free oligonucleotide.

3.5. DNaseI digestion assay

This study was performed to demonstrate the versatility and potential of SLN as a carrier for genetic material irrespective of whether it is susceptible/resistant to nuclease. Therefore, a primer susceptible to nuclease digestion was tested instead of MBO-asGCS, which is resistant to nucleases by design. When treated with DNaseI, SLNs were found to protect the primer from DNaseI activity. This was confirmed by the appearance of intact band in the gel when the complex was treated with sodium lauryl sulfate (Fig. 6).

3.6. Stability of the MBO-asGCS SLN complexes

The stability of the MBO-asGCS SLN complexes at CTAB to MBO-asGCS ratio of 6:1 (w/w) with respect to size and zeta-potential was evaluated in Nanopure distilled water, 10% FBS in 150 mM NaCl, and in RPMI medium containing 10% FBS. Upon MBO-asGCS loading to SLN, significant increase in size and decrease in zeta-potential of the complex was found (Fig. 7). The size of MBO-asGCS SLN1 complex and MBO-asGCS SLN2 complex in distilled water, 10% FBS in 150 mM NaCl, RPMI with 10% FBS was 188.0, 200.4, 1005.7 nm and 169.5, 215.3, 322.1 nm, respectively (Table 2). The particle size of the SLN1 and SLN2 complexes in water and in 10% FBS in 150 mM NaCl was not significantly different, which indicated that both complexes were stable in these media. However, when the nanoparticles were placed in the RPMI medium with 10% FBS, the growth in particle size of SLN1 and SLN2 complexes was significantly different. While the particle size of the MBO-asGCS SLN1

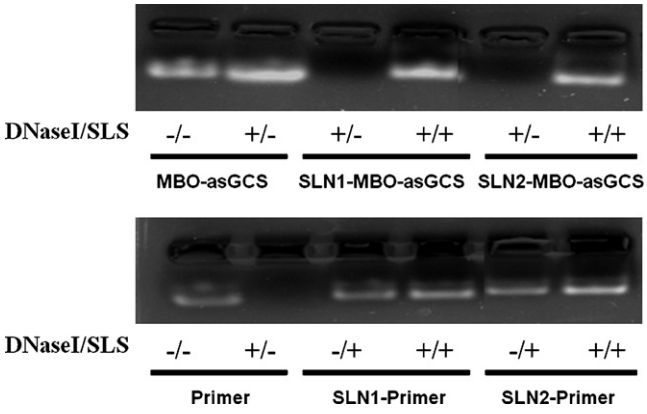

Fig. 6. Protection of the free and loaded oligonucleotide and primer against DNaseI degradation. MBO-asGCS is DNaseI resistant by design whereas the primer is susceptible to DNaseI degradation. After 30 min of incubation with DNaseI, SLS was added to displace the primer and the MBO-asGCS from the nanoparticles. +/− indicates the presence or absence of DNaseI or SLS.

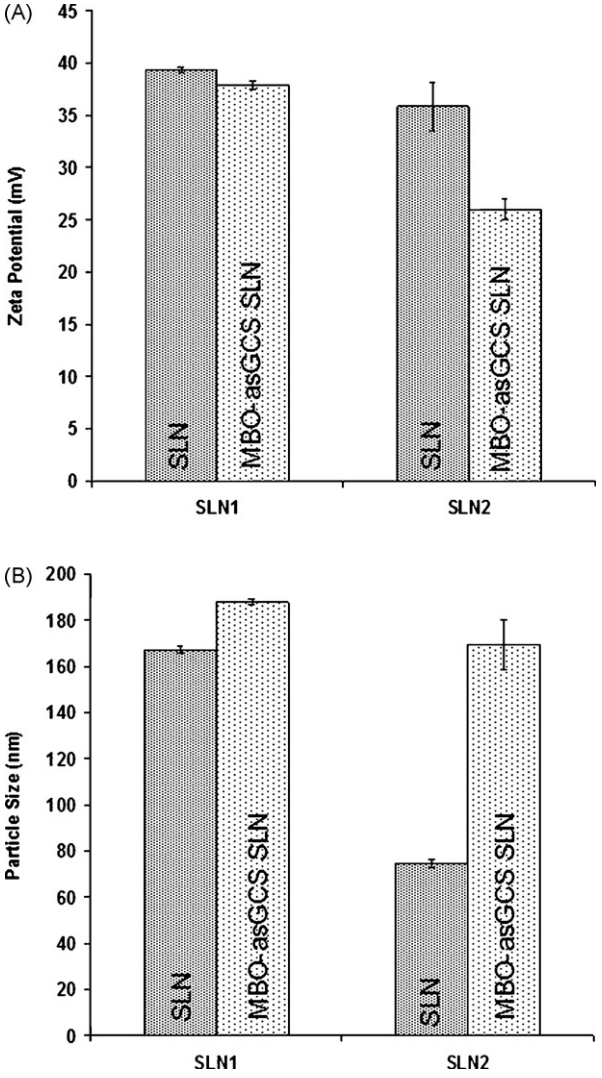

Fig. 7. Effect of MBO-asGCS loading onto SLN1 and SLN2 on (A) zeta-potential and (B) particle size of the resultant complex.

Table 2
Stability of the MBO-asGCS SLN complex in different media with respect to particle size, polydispersity index (PI) and zeta-potential at CTAB to MBO-asGCS-ratio of 6:1 (w/w).

Storage condition	SLN	Particle size (nm)* (mean ± SD)	PI (mean ± SD)	Zeta-potential (+mV) (mean ± SD)
Water	SLN1	188 ± 1.8	0.14 ± 0.009	37.85 ± 0.39
	SLN2	169.46 ± 10.94	0.40 ± 0.04	25.96 ± 1.02
10% FBS	SLN1	200.36 ± 2.34	0.27 ± 0.04	30.54 ± 2.52
	SLN2	215.26 ± 18.45	0.58 ± 0.05	10.83 ± 0.86
RPMI 10% FBS	SLN1	1005.7 ± 15.85	0.51 ± 0.02	n.d
	SLN2	322.1 ± 5.87	0.30 ± 0.03	n.d

* $p < 0.0001$, Alfa = 0.05.

complex increased to only 322 nm, the size of the SLN2 complex significantly increased to more than 1 μm (Fig. 8). The zeta-potential of SLN1 and SLN2 complexes in water and 10% FBS was (+) 37.9, 30.5 mV and 26.0, 10.8 mV, respectively.

3.7. Release of MBO-asGCS from the MBO-asGCS SLN complexes

The release of MBO-asGCS from the SLN complex at a CTAB to MBO-asGCS ratio of 6:1 (w/w) was evaluated in 150 mM NaCl, 10% lactose, and 10% FBS in 150 mM NaCl. Complex stability in 150 mM NaCl and 10% lactose was performed to identify a suitable vehicle for injection as reported by Cui and Mumper (2002a,b). After 30 min of incubation in the media, the complexes were found to be stable with no MBO-asGCS release as confirmed by gel electrophoresis (data not shown). Similarly, no release was observed when the complexes were stored at three physiological pHs (7.4, 7.2 and 4.5), representing the pH of the blood, cytoplasm, and lysosomes, respectively.

3.8. Cell viability assay

Oligo-free SLN1 and SLN2 were investigated for their non-specific toxicity against NCI/ADR-RES human ovary cancer cells (Fig. 9). Approximately 88% of the cells were viable when treated with SLN1 and SLN2 at CTAB concentration as high as 1.37 μM. After optimizing the MBO-asGCS SLN complex, the specific toxicity of the nanoparticles resulting from the activity of MBO-asGCS was evaluated against NCI/ADR-RES human ovary cancer cells (Fig. 10). Lipofectamine™ or lipofectamine-MBO-asGCS complex with or without 5 μM doxorubicin were taken as positive controls. Cells without any treatment were taken as negative control. ANOVA and Bonferroni tests were employed to interpret the differences in the level of cytotoxicity produced by different treatments. Naked MBO-asGCS, doxorubicin, and MBO-asGCS/doxorubicin mixture had insignificant effect on cell viability when compared to blank (oligo free) nanoparticles. Loading MBO-asGCS onto lipofectamine or SLN; however, significantly lowered cell viability. When MBO-asGCS loaded on lipofectamine, SLN1, or SLN2 were compared, significant difference in percent cell-viability was observed (p-value < 0.05). The percentage of viable cells after treatment with lipofectamine MBO-asGCS, MBO-asGCS SLN1, and MBO-asGCS SLN2 was 72, 61, and 56%, respectively, which is significantly lower than the percent cell viability of naked MBO-asGCS. Reduction in cell viability could only be attributed to the enhanced internalization of MBO-asGCS, which was brought about by its loading onto nanoparticles. This was further confirmed by the insignificant effect of nanoparticles loaded with scrambled oligonucleotides on cell viability. In order to corroborate the hypothesis that translational blockade of GCS by MBO-asGCS sensitized the NCI/ADR-RES human ovary cancer cells towards doxorubicin, cells were concurrently treated with the complexes and 5 μM doxorubicin. Significant differences were found when the percent cell viability amongst lipofectamine, SLN1, and SLN2 complexes in the presence of doxorubicin were compared (p-value < 0.05). The percent cell viability with lipofectamine, SLN1, and SLN2 complexes in the presence of doxorubicin was 46, 15, and 9%, respectively.

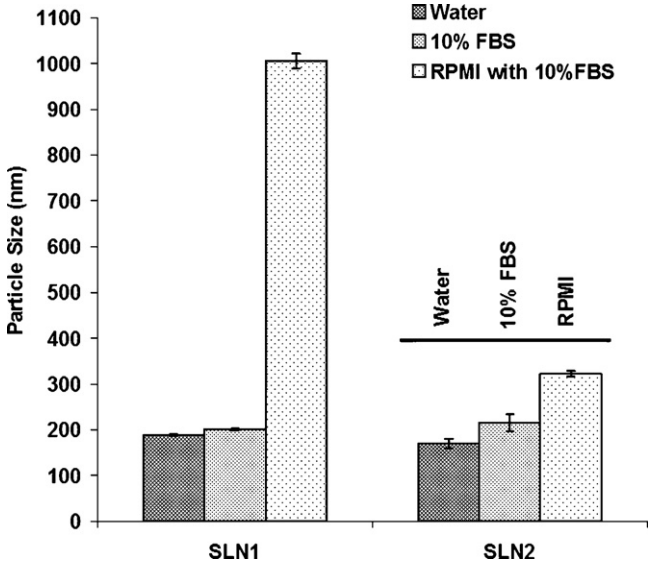

Fig. 8. Effect of water, FBS, and RPMI medium on the stability of the MBO-asGCS SLN1 and SLN2 complexes.

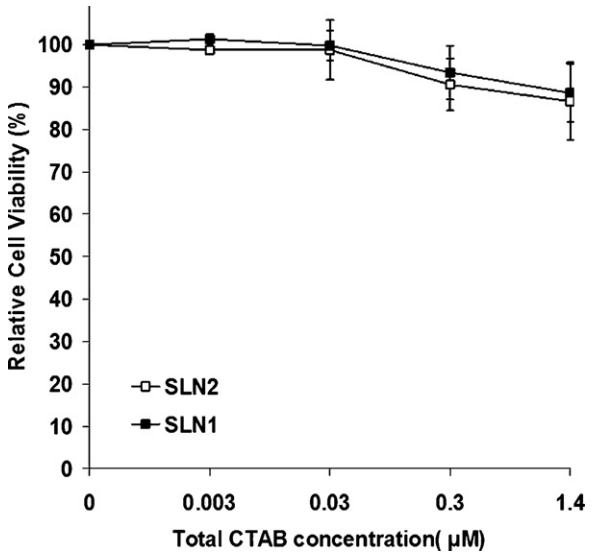

Fig. 9. Non-specific cytotoxicity of SLN1 and SLN2 on NCI/ADR-RES human ovary cancer cells at different CTAB concentrations.

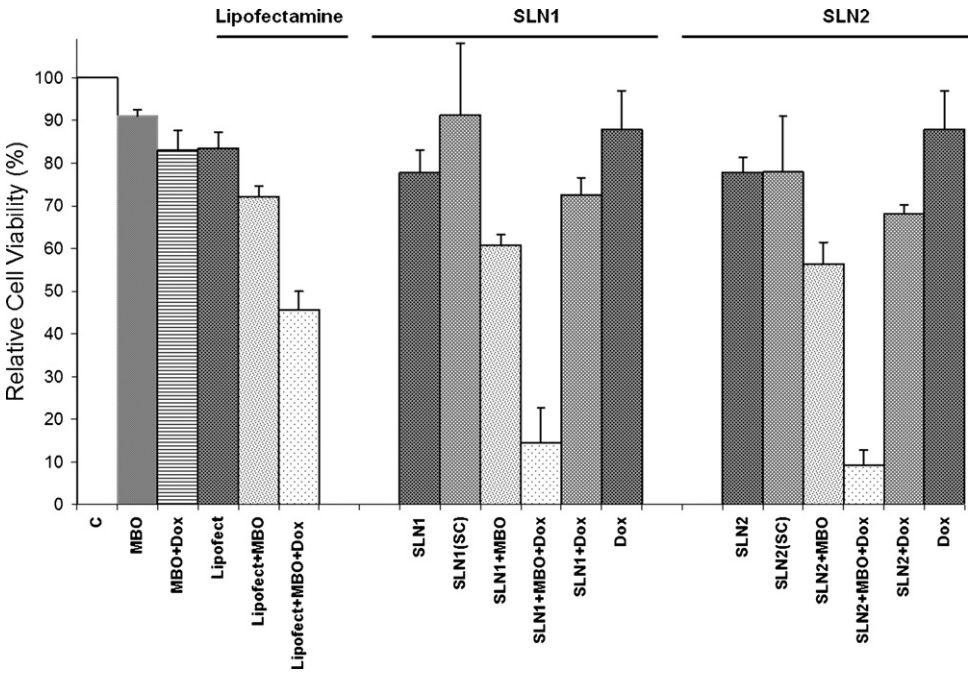

Fig. 10. Anticancer effects of free and bound MBO-asGCS to lipofectamine, SLN1, and SLN2 in the presence or absence of doxorubicin on NCI/ADR-RES human ovary cancer cells. Viable cell number was determined using the CellTiter-Glo luminescent assay. Vertical bars indicate the mean cell count + SEM ($n = 6$).

4. Discussion

Chemotherapy of cancer by cytotoxic drugs such as doxorubicin frequently leads to the development of MDR. Recent findings in the cause of MDR pointed to the over-expression of GCS, which converts ceramide into glucosylceramide (Gouaze et al., 2004). Ceramide was shown to act as a second messenger of numerous cell surface stimuli and plays a critical role in cell proliferation and apoptosis (Bleicher and Cabot, 2002; Cabot et al., 1999; Liu et al., 2008). Therefore, down-regulating GCS using antisense approach was considered a viable option to overcome MDR (Liu et al., 2008). This option however is fraught with delivery challenges, which include nuclease sensitivity, target affinity, toxicity, and delivery (Weyermann et al., 2004). Although some of these problems were partially or completely solved by modification in the oligonucleotide backbone, the two prominent concerns remaining are toxicity and delivery. These challenges could be addressed by loading the MBO-asGCS onto cationic SLN. This assumption was confirmed in recent studies that evaluated SLN as a potential carrier of genetic material (Bondi et al., 2007).

In the present study a modified microemulsion method applying shear homogenization and sonication was used for the preparation of SLN made from stearyl alcohol or stearyl alcohol/ceramide VI at 1:1 ratio as the core lipid. Since naturally occurring C-18 to 24 ceramide found at physiological levels had an established role in cell apoptosis (Stover et al., 2005), our group envisioned a similar apoptotic potential of phyto-ceramide with similar number of carbon chain. However, when evaluated in cytotoxicity studies, ceramide VI solution was found to be non-toxic against NCI/ADR-RES human ovary cancer cells (data not shown). The particle size of the nanoparticles was however significantly reduced ($p < 0.0001$) when 50% of stearyl alcohol was substituted with ceramide IV. The reduction in particle size by half when compared to SLN1 could be attributed to the three hydroxyl group present in ceramide VI (Fig. 1). These hydrophilic groups are projected on the particle surface where they allow the formation of a static layer of water around the particle. Water held around particle surface complemented with cationic charge of the well-inserted CTAB would contribute to the formation of smaller particles than SLN1 where only one hydroxyl group per molecule is contributing towards the formation of such barrier. Therefore, larger number of stearyl alcohol molecules in SLN1 coalesces to form a stable particle leading to a larger particle size. Nonetheless, both formulations had comparable zeta-potential and a polydispersity index around 0.2, which indicates narrow particle size distribution. A similar observation was reported by Cui and Mumper (2002a,b) who observed a reduction in particle size when DOPE (dioleoyl phosphatidylethanolamine) was added to cationic nanoparticles made from emulsifying wax and CTAB.

Stability studies of the formulations were performed to investigate the effect of temperature on particles size during storage. Therefore, formulations were placed in open light at controlled room temperature, in refrigeration, and at 37 °C. Both formulations were stable when refrigerated and when stored at controlled room temperature. However, a significant growth in SLN1 particle size was observed when the sample was stored at 37 °C, which might have resulted from enhanced interparticle collision and aggregation (Freitas and Müller, 1999). No significant increase in particle size was observed with SLN2 due to the presence of hydrostatic barrier around the particle, which was formed by the hydroxyl groups in ceramide VI and cetyl alcohol. The electrostatic repulsive and hydrostatic barrier around the particle appeared to be adequate enough to repel the impulse of the incoming particle with higher acceleration due to the higher temperature.

SLN formulations were also shown to have a similar non-specific toxicity against NCI/ADR-RES human ovary cancer cells as Lipofectamine™. Once the non-specific toxicity was ascertained, SLN1 and SLN2 were subjected to binding studies. Binding oligonucleotides to a carrier was shown to reduce toxicity and enhance the intracellular accumulation of oligonucleotides via endocytosis (Bondi et al., 2007). MBO-asGCS SLN complexes were formed by mixing a fixed concentration of MBO-asGCS with variable quantity of the nanoparticles. These complexes were first screened by measuring zeta-potential as a function of CTAB concentration. Since zeta-potential is the potential between shear planes and the medium, it decreases as the charge on the surface is neutralized as a result of MBO-asGCS binding. The objective of generating this profile was to predict the optimal binding ratio between MBO-asGCS

and SLN. Based on the zeta-potential profile, complete binding was predicted to occur at a CTAB to MBO-asGCS ratio between 1.25:1 and 10:1 (w/w), which was confirmed by gel electrophoresis.

Before proceeding to the cell viability studies, the stability of the optimized complexes was evaluated in RPMI culture medium and was compared to the stability of the nanoparticles in water and a simple medium made of 10% FBS in 150 mM NaCl. Both SLN1 and SLN2 complexes were stable in water and in 10% FBS. However, MBO-asGCS SLN1 complex significantly increased in size to above 1 μm when placed in RPMI medium whereas MBO-asGCS SLN2 complex maintained a particle size of approximately 300 nm. Maintaining particle size less than 300 nm was desirable to minimize RES clearance (Lutz et al., 1989). The increase in SLN1 complex size in RPMI medium could be due to the interaction between the cationic SLN and the in/organic anion in the medium. This increase was smaller in SLN2 due to its lower zeta-potential, which was attributed to the presence of a hydrostatic layer around the particle surface brought about by ceramide VI.

After characterizing MBO-asGCS SLN complexes, their ability to protect and release the bound oligonucleotide was investigated. Since MBO-asGCS is a mixed backbone oligonucleotide designed to be resistant to nuclease action, a primer whose phosphodiester bond between nucleotide is susceptible to nuclease action was tested. The free primer was digested by the DNaseI within 30 min of incubation whereas the bound primer did not. To verify the existence of a primer–SLN complex, the primer was displaced from nanoparticles by the negatively charged SLS. The presence of a free primer was subsequently confirmed by gel electrophoresis. These data suggested that SLN has the ability to protect the oligonucleotide from nucleases. Furthermore, the bonding between MBO-asGCS and SLN is expected to remain intact after administration until the SLN reaches the cytoplasm where the MBO-asGCS must be released for antisense action. To study the release of the MBO-asGCS, the complexes were allowed to stand in 10% lactose, 10% FBS in 150 mM NaCl, and in 150 mM NaCl for 30 min. Similarly, the release of the MBO-asGCS from the complexes at pH 4.5, 7.2, and 7.4 was evaluated to investigate whether the MBO-asGCS would be released at conditions simulating intra or extracellular environment. At the conclusion of the experiments it was found that the MBO-asGCS was not released from the complexes indicating that the stability of the complexes was retained in the tested media. Also, the complexes at cytoplasmic (pH 7.2) and lysosomal (pH 4.5) conditions did not release the MBO-asGCS, which was contrary to our expectation. Whereas we included only one intracellular factor into consideration, the release of MBO-asGCS from the complex might be governed by more than one intracellular factors, for example, enzyme, ions etc. Therefore, to indirectly investigate this assumption, the sensitivity of the cells to MBO-asGCS SLN complexes, with or without the addition of 5 μM doxorubicin, was evaluated against NCI/ADR-RES human ovary cancer cells. The selection of the cell lines and the concentration of MBO-asGCS and doxorubicin in this study were based on the outcome of previous studies in which the effect of MBO-asGCS was examined in adriamycin resistant and sensitive cells (NCI/ADR-RES, MCF-7, EMT6/AR1, and EMT6). When healthy cells were treated with the oligonucleotide, no significant reduction in the level of GCS was found, whereas in resistant cells, oligonucleotide significantly reduced the level of GCS. Uptake of the MBO-asGCS in adriamycin resistant and sensitive cells (NCI/ADR-RES and MCF-7), however, was found to be similar (Patwardhan et al., 2009). Furthermore, the effect of asGCS ODN-7, which has the same sequence and specificity as MBO-asGCS, was evaluated in different cell lines. Its effect on adriamycin resistant cells (MCF-7 AdrR (NCI/ADR-RES)) and normal human mammary epithelial cells (HMEC) was found to be insignificant (Liu et al., 2004). asGCS ODN-7 however had a dose dependent effect on MCF7-AdrR (NCI/ADR-RES) breast cancer cells, which was confirmed by a dose dependent decrease in the level of GCS mRNA as measured by RT-PCR. Furthermore, asGCS ODN-7 significantly increased doxorubicin toxicity in adriamycin resistant cells in comparison to sensitive and normal cells (Liu et al., 2004).

In this study, lipofectamine-MBO-asGCS complex was taken as a positive control. Employing Bonferroni multiple comparison test, MBO-asGCS complexes with SLN1, SLN2, or lipofectamine, were found to significantly reduce cell viability when compared to naked MBO-asGCS. This reduction in cell viability may be attributed to the improved internalization of the MBO-asGCS whose antisense action resulted in enhanced intracellular concentration of ceramide and apoptosis. Since the NCI/ADR-RES human ovary cancer cells are resistant to doxorubicin no significant change in cells viability was observed when cell were treated with doxorubicin or doxorubicin/MBO-asGCS solutions. However, a three-fold decrease in viability was observed when the cells were concurrently treated with the MBO-asGCS complexes and 5 μM of doxorubicin. The increase in the sensitivity of the cells to doxorubicin in the presence of MBO-asGCS complexes might be due to the reversal in cell resistance as a result of ceramide accumulation. MBO-asGCS is a second generation mixed backbone oligonucleotide, which was designed to downregulate the production of glucosylceramide synthase (GCS) in adriamycin resistant cells. Downregulation of GCS was found to increase the sensitivity of the cells to doxorubicin (Liu et al., 2004). Although these preliminary data displayed enhanced efficacy of complex with and without doxorubicin, the exact mechanism about their transport and intracellular trafficking/release need further investigation.

5. Conclusion

In this study it was shown that down-regulating GCS gene expression with the use of asGCS sensitizes the cells to doxorubicin. These results are in line with the previously reported studies on the therapeutic effects of asGCS. A delivery vehicle such as SLN is however required for the internalization of the oligonucleotide. asGCS bound to SLN significantly reduced the viability of the NCI/ADR-RES human ovary cancer cells in the presence of doxorubicin. The resistance of cancer cells to doxorubicin was attributed to the upregulations of the GCS gene expression (Liu et al., 2008). While additional studies are required to further our understanding of the mechanisms by which MBO-asGCS SLN complexes work, the preliminary results reported in this study are marked evidence on the potential use of asGCS SLN complexes in the treatment and/or management of tumors resistant to chemotherapy. The potential benefits of SLN may also be attributed to their favorable physical properties, stability profile, and their ability to protect the genetic material from DNAse activity. While traditional SLN are less stable at higher storage temperatures and in RPMI medium, the addition of ceramide to the composition of the SLN was shown to stabilize the nanoparticles in these media. Ceramide however did not induce apoptosis. Nonetheless, its use in SLN was shown to lower particle size and enhances the stability of the nanoparticles. Therefore, the use of ceramides in the preparation of SLN warrants further studies to elucidate its full potential.

Acknowledgments

This work was partially supported by the United State Public Health Service/NIH grant P20 RR16456 from the National Center of Research Resources (Y.Y.L).

References

Asasutjarit, R., Lorenzen, S., Sirivichayakul, S., Ruxrungtham, K., Ruktanonchai, U., Ritthidej, G.C., 2007. Effect of solid lipid nanoparticles formulation composition

on their size, zeta-potential and potential for *in vitro* pHIS-HIV-Hugag transfection. Pharm. Res. 24, 1098–1107.
Bijsterbosch, M.K., Manoharan, M., Dorland, R., Veghel, R.V., Biessen, E.A.L., Berkel, T.J.C.V., 2002. Bis-cholesteryl-conjugated phosphorothioate oligodeoxynucleotides are highly selectively taken up by the liver. J. Pharmacol. Exp. Therapeut. 302, 619–626.
Bleicher, R.J., Cabot, M.C., 2002. Glucosylceramide synthase and apoptosis. Biochim. Biophys. Acta (BBA)-Mol. Cell Biol. Lipids 1585, 172–178.
Bondi, L.M., Azzolina, A., Craparo, E.F., Lampiasi, N., Capuano, G., Giammona, G., Cervello, M., 2007. Novel cationic solid-lipid nanoparticles as non-viral vectors for gene delivery. J. Drug Target. 15, 295–301.
Cabot, M.C., Giuliano, A.E., Han, T.Y., Liu, Y.Y., 1999. SDZ PSC 833, the cyclosporine A analogue and multidrug resistance modulator, activates ceramide synthesis and increases vinblastine sensitivity in drug-sensitive and drug-resistance cancer cells. Cancer Res. 59, 880–885.
Cui, Z.R., Mumper, R.J., 2002a. Genetic immunization using nanoparticles engineered from microemulsion precursors. Pharm. Res. 19, 939–946.
Cui, Z.R., Mumper, R.J., 2002b. Topical immunization using nanoengineered genetic vaccines. J. Control. Release 81, 173–184.
Freitas, C., Müller, R.H., 1999. Correlation between long-term stability of solid lipid nanoparticles (SLN™) and crystallinity of the lipid phase. Eur. J. Pharm. Biopharm. 47, 125–132.
Grünweller, A., Gillen, C., Erdmann, V.A., Kurreck, J., 2004. Cellular uptake and localization of a Cy3-labeled siRNA specific for the serine/threonine kinase Pim-1. Oligonucleotides 13, 345–352.
Gouaze, V., Liu, Y.Y., Prickett, C.S., Yu, J.Y., Giuliano, A.E., Cabot, M.C., 2005. Glucosylceramide synthase blockade down-regulates P-glycoprotein and resensitizes multidrug-resistant breast cancer cells to anticancer drugs. Cancer Res. 65, 3861–3867.
Gouaze, V., Yu, J.Y., Bleicher, R.J., Han, T.Y., Liu, Y.Y., Wang, H., Gottesman, M.M., Bitterman, A., Giuliano, A.E., Cabot, M.C., 2004. Overexpression of glucosylceramide synthase and P-glycoprotein in cancer cells selected for resistance to natural product chemotherapy. Mol. Cancer Ther. 3, 633–639.
Gouaze-Andersson, V., Cabot, M.C., 2006. Glycosphingolipids and drug resistance. Biochim. Biophys. Acta 1758, 2096–2103.
Hatziantoniou, S., Deli, G., Nikas, Y., Demetzos, C., Papaioannou, G., 2007. Scanning electron microscopy study on nanoemulsion and solid lipid nanoparticles containing high amounts of ceramides. Micron 38, 819–823.
Leonetti, C., Biroccio, A., Benassi, B., Stringaro, A., Stoppacciaro, A., Semple, S.C., Zupi, G., 2001. Encapsulation of c-myc antisense oligonucleotides in lipid particles improves antitumoral efficacy *in vivo* in a human melanoma line. Cancer Gene Ther. 8, 459–468.
Liu, Y.Y., Yu, J.Y., Yin, D., Patwardhan, G.A., Gupta, V., Hirabayashi, Y., Holleran, W.M., Giuliano, A.E., Jazwinski, S.M., Gouaze-Andersson, V., Consoli, D.P., Cabot, M.C., 2008. A role for ceramide in driving cancer cell resistance to doxorubicin. FASEB J. 22, 2541–2551.
Liu, Y.Y., Han, T.Y., Giuliano, A.E., Cabot, M.C., 1999. Expression of glucosylceramide synthase, converting ceramide to glucosylceramide, confers adriamycin resistance in human breast cancer cells. J. Biol. Chem. 274, 1140–1146.
Liu, Y.Y., Han, T.Y., Giuliano, A.E., Cabot, M.C., 2001. Ceramide glycosylation potentiates cellular multidrug resistance. FASEB J. 15, 719–730.
Liu, Y.Y., Han, T.Y., Giuliano, A.E., Hansen, N., Cabot, M.C., 2000. Uncoupling ceramide glycosylation by transfection of glucosylceramide synthase antisense reverses adriamycin resistance. J. Biol. Chem. 275, 7138–7143.
Liu, Y.Y., Han, T.Y., Yu, J.Y., Bitterman, A., Le, A., Giuliano, A.E., Cabot, M.C., 2004. Oligonucleotides blocking glucosylceramide synthase expression selectively reverse drug resistance in cancer cells. J. Lipid Res. 45, 933–940.
Lucci, A., Han, T.Y., Giuliano, A.E., Cabot, M.C., 1999. Multidrug resistance modulators and doxorubicin synergize to elevate ceramide levels and elicit apoptosis in drug-resistant cancer cells. Cancer 86, 300–311.
Lutz, O., Meraihi, Z., Mura, J.L., Frey, A., Riess, G.H., Bach, A.E., 1989. Fat emulsion particle size: influence on the clearance rate and the tissue lipolytic activity. Am. J. Clin. Nutr. 50, 1370–1381.
Montana, G., Bondi, B.L., Carotta, R., Picone, P., Craparo, E.F., San Biagio, P.L., Giammona, G., Carlo, M.D., 2007. Employment of cationic solid-lipid nanoparticles as RNA carriers. Bioconjug. Chem. 18, 302–308.
Norris-Cervetto, E., Butters, T.D., Dwek, R.A., Callaghan, R., Platt, F.M., 2004. Inhibition of glucosylceramide synthase does not reverse drug resistance in cancer cells. J. Biochem. 279, 40412–40418.
Olbrich, C., Bakowsky, U., Lehr, C.-M., Müller, R.H., Kneuer, C., 2001. Cationic solid-lipid nanoparticles can efficiently bind and transfect plasmid DNA. J. Control. Release 77, 345–355.
Patwardhan, G.A., Zhang, Q.J., Yin, D., Gupta, V., Bao, J., Senkal, C.E., Ogretman, B., Cabot, M.C., Shah, G.V., Sylvester, P.W., Jazwinski, S.M., Liu, Y.Y., 2009. A new mixed backbone oligonucleotide against glucosylceramide synthase sensitizes multidrug-resistant tumors to apoptosis. PLosONE 4, 1–11.
Pozo-Rodríguez, A.D., Delgado, D., Solinís, M.A., Gascón, A.R., Pedraz, J.L., 2007. Solid lipid nanoparticles: formulation factors affecting cell transfection capacity. Int. J. Pharm. 339, 261–268.
Stover, T.C., Sharma, A., Robertson, G.P., Kester, K., 2005. Systemic delivery of liposomal short-chain ceramide limits solid tumor growth in murine models of breast adenocarcinoma. Clin. Cancer Res. 11, 3465–3474.
Tabatt, K., Kneuer, K., Sameti, M., Olbrich, C., Müller, R.H., Lehr, C.M., Bakowsky, U., 2004a. Transfection with different colloidal systems: comparison of solid lipid nanoparticles and liposomes. J. Control. Release 97, 321–332.
Tabatt, K., Sameti, M., Olbrich, C., Müller, R.H., Lehr, C., 2004b. Effect of cationic lipid and matrix lipid composition on solid lipid nanoparticles-mediated gene transfer. Eur. J. Pharm. Biopharm. 57, 155–162.
Vighi, E., Ruozi, B., Montanari, M., Battini, R., Leo, E., 2007. Re-dispersible cationic solid lipid nanoparticles (SLNs) freeze-dried without cryoprotectors: characterization and ability to bind the pEGFP-plasmid. Eur. J. Pharm. Biopharm. 67, 320–328.
Vogel, V., Lockmann, D., Weyermann, J., Mayer, G., Broek van den, J.A., Hasse, W., Wouters, D., Schubert, U.S., Kreuter, J., Zimmer, A., SChubert, D., 2005. Oligonucleotide–protamine–albumin nanoparticles: preparation, physical properties, and intracellular distribution. J. Control. Release 103, 99–111.
Weyermann, J., Lochmann, D., Zimmer, A., 2004. Comparison of antisense oligonucleotide drug delivery systems. J. Control. Release 100, 411–423.
Yessine, M., Meier, C., Petereit, H., Lerous, J., 2006. On the role of methacrylic acid copolymers in the intracellular delivery of antisense oligonucleotides. Eur. J. Pharm. Biopharm. 63, 1–10.